Identification of Carboxypeptidase E and γ-Glutamyl Hydrolase as Biomarkers for Pulmonary Neuroendocrine Tumors by cDNA Microarray

PING HE, MD, LYUBA VARTICOVSKI, MD, ELISE D. BOWMAN, MS, JUNYA FUKUOKA, MD, JUDITH A. WELSH, BS, KOH MIURA, MD, JIN JEN, PHD, EDWARD GABRIELSON, MD, ELISABETH BRAMBILLA, MD, WILLIAM D. TRAVIS, MD, AND CURTIS C. HARRIS, MD

Pulmonary neuroendocrine tumors vary dramatically in their malignant behavior. Their classification, based on histological examination, is often difficult. In search of molecular and prognostic markers for these tumors, we used cDNA microarray analysis of human transcripts against reference RNA from a well-characterized immortalized bronchial epithelial cell line, BEAS-2B. Tumor cells were isolated by laser-capture microdissection from primary tumors of 17 typical carcinoids, small cell lung cancers, and large cell neuroendocrine carcinomas. An unsupervised, hierarchical clustering algorithm resulted in a precise classification of each tumor subtype according to the proposed histological classification. Selection of genes, using supervised analysis, resulted in the identification of 198 statistically significant genes ($P < .004$) that also accurately discriminated between 3 predefined tumor subtypes. Two-by-two comparisons of these genes identified classifier genes that distinguished each tumor subtype from the others. Changes in expression of selected differentially expressed genes for each tumor subtype were internally validated by real-time reverse-transcription polymerase chain reaction. Expression of 2 potential classifier gene products, carboxypeptidase E (CPE) and γ-glutamyl hydrolase (GGH), was validated by immunohistochemistry and cross-validated on additional archival samples of pulmonary neuroendocrine tumors. Kaplan-Meier survival analysis revealed that immunostaining for CPE was a statistically significant predictor of good prognosis, whereas GGH expression correlated with poor prognosis. Thus, cDNA microarray analysis led to the identification of 2 novel biomarkers that should facilitate molecular diagnosis and further study of pulmonary neuroendocrine tumors. HUM PATHOL 35:1196-1209.

Key words: **atypical carcinoid, biomarkers, carboxypeptidase E, γ-glutamyl hydrolase, gene pulmonary neuroendocrine tumors.**

Abbreviations: **ABC, avidin-biotin-peroxidase complex; AC, atypical carcinoid; CPE, carboxypeptidase E; GGH, γ-glutamyl hydrolase; IHC, immunohistochemistry; LCM, laser capture microdissection; LCNEC, large cell neuroendocrine carcinoma; NE, neuroendocrine; PBS, phosphate-buffered saline; RT-PCR, reverse-transcription polymerase chain reaction; SCLC, small cell lung cancer; TC, typical carcinoid.**

Lung cancer continues to be the leading cause of cancer-related deaths worldwide. The high incidence and mortality reflect continued exposure to cigarette smoking, lack of effective methods for early diagnosis, and inadequate markers of aggressive lung cancer types. Pulmonary neuroendocrine (NE) tumors account for 20% to 30% of lung cancer cases and include low-grade typical carcinoid (TC), intermediate-grade atypical carcinoid (AC), high-grade large cell neuroendocrine carcinoma (LCNEC), and small cell lung cancer (SCLC).[1] TC, AC, and LCNEC collectively comprise only 3%-5% of all pulmonary malignancies, whereas SCLC accounts for 15%-25%. The prognostic relevance of pulmonary NE tumors has changed substantially since the recognition of the LCNEC subtype,[2] because pulmonary NE tumors vary significantly in their malignant behavior. The 5-year survival rates for TC, AC, LNEC, and SCLC are 87%, 56%, 27%, and 9%, respectively. These tumors have a similar morphological appearance, with organoid, trabecular or rosette-like patterns, and common neuroendocrine markers detectable by immunohistochemistry: chromogranin A, synaptophysin, and neural cell adhesion molecule (NCAM, CD56). In some cases, electron microscopy analysis is also required for the detection of neuroendocrine granules. The current treatment for patients with TC and AC is surgical resection, because these tumors grow relatively slowly and are frequently detected as solitary pulmonary lesions. Surgical resection is feasible in less than 1/3 of LCNEC patients with or without neoadjuvant treatment.[3] Unfortunately, at the time of diagnosis, the vast majority of SCLC is disseminated, and prognosis is poor. Thus, accurate and

From the Laboratory of Human Carcinogenesis, National Cancer Institute, National Institutes of Health, Bethesda, MD; Department of Pulmonary and Mediastinal Pathology, Armed Forces Institute of Pathology, Washington, DC, USA; Division of Hematology, Center for Biologics Evaluation and Research, Food and Drug Administration, Bethesda, MD, USA; Department of Surgery, Tohoku University Postgraduate School of Medicine, Sendai, Japan; Laboratory of Population Genetics, National Cancer Institute, National Institutes of Health, Bethesda, MD, USA; Department of Pathology, Johns Hopkins University, Baltimore, MD USA; and Laboratory of Cellular Pathology, Grenoble, France. Accepted for publication June 18, 2004.

Address correspondence and reprint requests to Curtis C. Harris, MD, Chief, Laboratory of Human Carcinogenesis, National Cancer Institute, National Institutes of Health, 37 Convent Drive, Bldg. 37, Rm. 3068, Bethesda, MD 20892-4255.

0046-8177/$—see front matter

doi:10.1016/j.humpath.2004.06.014

timely diagnosis of pulmonary NE tumor subtypes is essential for the selection of appropriate treatment and prediction of clinical outcome.

DNA microarray technology provides a powerful tool for analyzing changes in gene expression.[4,5] Application of this technology to human lung cancer facilitates the characterization of gene expression profiles.[6-10] However, very few have led to the identification of molecular markers that can aid in the diagnosis and prognosis of lung cancer. There are no molecular markers that distinguish among the subtypes of pulmonary NE tumors. In addition, the generation of a genome-wide expression profile requires a large dataset with multiple samples. This is difficult to obtain for many primary tumors, especially those that rarely undergo an open resection, including SCLC.

Using laser capture microdissection (LCM)[11] and cDNA microarray from a limited number of pulmonary neuroendocrine tumor samples, we have identified 198 genes that are differentially expressed in pulmonary NE tumors by comparing tumor gene expression profiles with a reference RNA from a human immortalized bronchopulmonary cell line with NE features. The RNA changes of 2 candidate genes, CPE and GGH, were cross-validated by immunohistochemistry (IHC) on 55 cases of pulmonary NE tumors, and their expression was correlated with clinical outcome.

MATERIALS AND METHODS

Tissue Samples

Fresh-frozen tissues of 17 primary pulmonary NE tumors (11 TC, 2 LCNEC, 3 SCLC, and 1 with combined features of SCLC and LCNEC) were collected from hospitals in Baltimore and Maryland metropolitan areas over an 11-year period. Tissues were flash-frozen after surgery and stored at −80°C until used. Histopathologic classification of these tumors was based on the 1999 World Health Organization/LASLSC "histological typing of lung and pleural tumors" proposed by Travis et al.[1,2] Additional samples used for IHC were obtained from the Laboratory of Cellular Pathology, Grenoble, France and the Department of Pathology, Johns Hopkins University, Baltimore, MD. A total of 68 cases (29 TC, 5 AC, 9 LCNEC, and 25 SCLC) were used for IHC; of these, 55 cases generated informative data. Fifty-four of those 55 cases have clinical data that were used for Kaplan-Meier survival analysis.

Laser Capture Microdissection

Frozen tissue (.5 × .5 × .5 cm) was embedded in OCT in a cryomold and immersed immediately in dry, ice-cold 2-methylbutane at −50°C. Tissue sections (8 μm) were mounted on Silane-coated slides and kept at −80°C until use. The slides were fixed by immersion in 70% ethanol, stained with hematoxylin and eosin and air-dried for 10 minutes after xylene treatment.

The PixCell LCM system was used for LCM. Tumor cells were fused to transfer film by thermal adhesion after laser pulse and transferred into tubes for RNA extraction (Fig 1).Total RNA was extracted using Micro RNA isolation kit (Stratagene, La Jolla, CA) according to the manufacturer's instructions. RNA quality was evaluated by spectrophotometry and gel electrophoresis. Purified RNA was dissolved into 11 μL of diethyl polycarbonate–treated water and used for amplification. The amplified RNA was subjected to cDNA microarray analysis.

Tissue Culture

The reference cell line, BEAS-2B, derived from normal human bronchial epithelium, was immortalized by SV40.[12] Cells were cultured in a serum-free medium, LHC-9, and harvested at passage 30. Total RNA was isolated from cultured cells using the Micro RNA isolation kit (Stratagene) according to the manufacturer's instructions.

RNA Amplification

RNA amplification was performed as described by Luo et al.[13] Briefly, oligo (dT) primers with T7 promoter sequence, 5'-TCTAGTCGACGGCCAGTGAATTGTAATACGAC-TCAC-TATAGGGCG$(T)_{21}$-3', were used to synthesize the first strand of cDNA. After the second strand of cDNA synthesis, RNA was amplified using T7 RNA polymerase on the cDNA templates. Two rounds of amplification, starting with 1 μg of total RNA, generated 40 to 60 μg of amplified RNA, which was used for microarray analysis.

Microarray, Hybridization, and Analysis

The cDNA microarray contained 9180 cDNA clones based on the Hs Unigene build #131 platform. This total comprised 7102 "named" genes, 1179 expressed sequence tag (EST) clones, and 122 Incyte clones per slide. The slides were printed by the National Cancer Institute (NCI) Microarray Facility, Advanced Technology Center, Gaithersburg, MD. RNA (8 μg), amplified from the BEAS-2B reference cell line, was labeled with Cy5-dUTP. Amplified RNA (4 μg each) from tumors was labeled with Cy3-dUTP using Superscript II (Invitrogen, Carlsbad, CA). Briefly, RNA was incubated with Cy3-dUTP or Cy5-dUTP (Perkin Elmer Life Sciences, Boston, MA) at 42°C for 1 hour to synthesize the first strand cDNA. The reaction was stopped by the addition of 5 μL .5 mmol EDTA, and the RNA was degraded by the addition of 10 μL 1N NaOH and then incubated at 65°C for 1 hour. After neutralizing, the samples were purified by Microcon 30 (Millipore, Bedford, MA). Each pair of labeled samples was hybridized to DNA on slides at 65°C for 16 hours, and the acquired image was processed with GenePix Pro 3.0 software (Axon Instruments, Union City, CA). The basic raw data and derived ratio measurements were then uploaded to the NCI's MicroArray Database system for normalization and data extraction in formats compatible with microarray analysis tools. Overall quality of arrays by visual inspection, signal-to-background ratios, spot size, and intensity filters were applied to each sample. Hybridization quality replicates in 6 samples were performed using the same probes on a different day for quality control of microarray labeling, hybridization reproducibility, and consensus expression data (>95% Pearson coefficient correlation between the replica slides). For unsupervised analysis of expression trends across all samples, genes were selected based on normalized Cy5:Cy3 ratios and then subjected to hierarchical clustering analysis, using CLUSTER and TREEVIEW software.[14] For supervised analysis, hierarchical clustering and gene selection were performed using the class comparison tTool, which is part of the microarray analysis software BRB-ArrayTools, version 3.0 (NCI, Bethesda MD; available at *http://linus.nci.nih.gov/brb*).

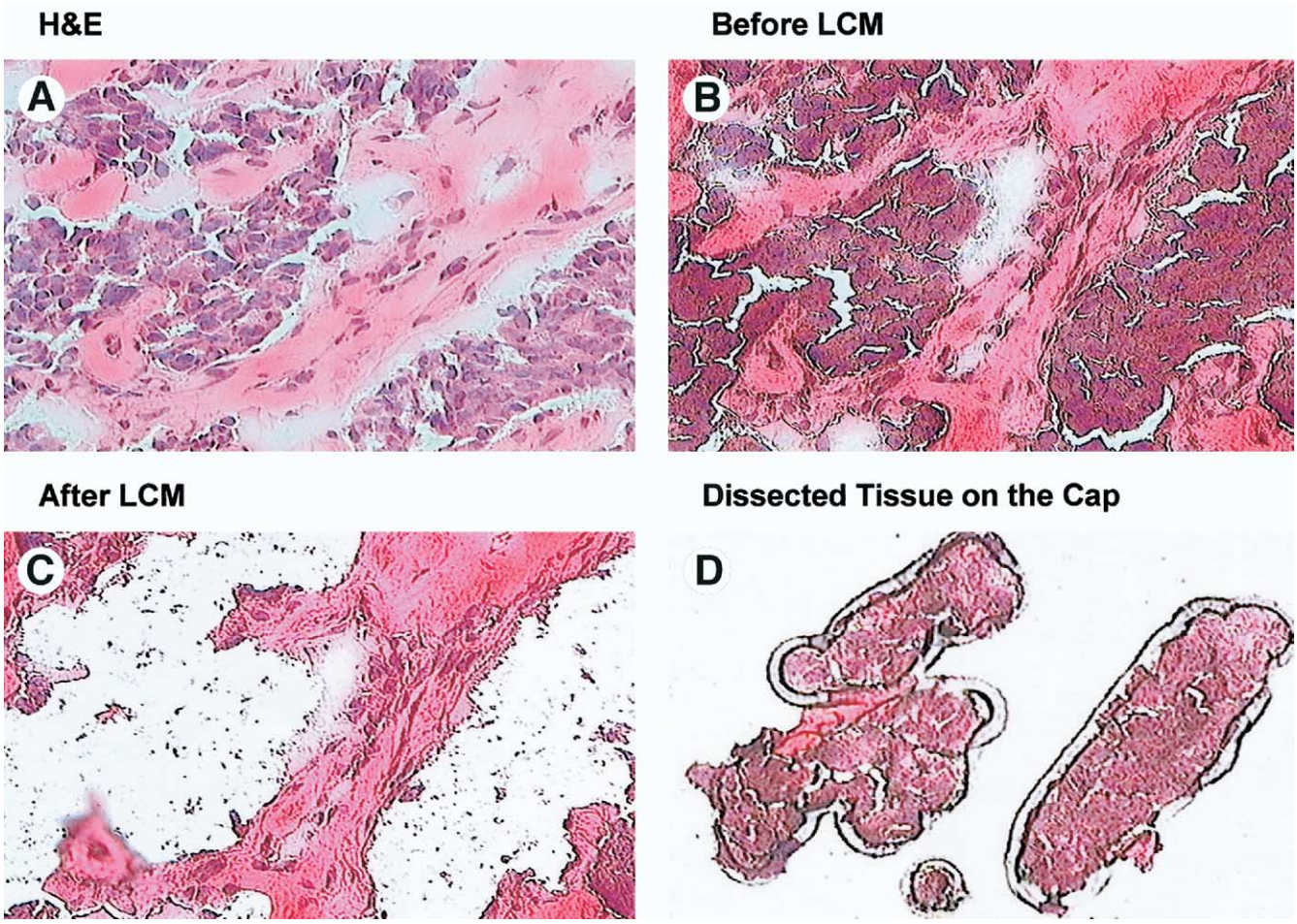

FIGURE 1. LCM of cancer cells. (A) Hematoxylin and eosin stain of a frozen section of TC tissue with characteristic carcinoid cell nests and stroma infiltration. (B) Air-dried section before LCM. (C) The remaining tissue after LCM. (D) Tumor cells captured by LCM on a thermal plastic cap for retrieval.

Based on univariate *F*-tests, we identified genes differentially expressed between tumor samples and reference RNA.

Real-Time PCR

Total RNA was purified from a new sample extracted from tumors by LCM, using the Stratagene Absolutely RNA microprep kit. Samples were treated by DNase I to eliminate DNA contamination. Primers were designed, using Primer Express Software, version 1.5 (Applied Biosystems, Foster City, CA) based on sequences from GenBank and purchased from Biosource International (Camarillo, CA). Final probe concentration was 200 nmol for each gene. Endogenous 18s RNA (Applied Biosystems) was used as an internal reference. Reverse transcription was completed with the RT-EZ RNA kit (Applied Biosystems) according to the manufacturer's instructions. Samples were run in triplicate and monitored on the ABI PRISM 7700. Quantitation was based on levels determined in the BEAS-2B cell line RNA for each gene.

Immunohistochemistry

Immunohistochemistry was performed by the avidin-biotin-peroxidase complex (ABC) method (Vectastain Elite ABC kit; Vector Laboratories, Foster City, CA). Briefly, slides were deparaffinized and rehydrated through xylene and alcohol in Coplin jars. Endogenous peroxidase was blocked with 3% H_2O_2 in phosphate-buffered saline (PBS) for 20 minutes. Unless otherwise mentioned, washes were in PBS at room temperature. After 2 washes, heat-induced epitope retrieval was performed in a citrate buffer (pH 6.0) in a Biocare medical chamber (Walnut Creek, CA). Slides were rinsed, and the edge of a tissue section was circled with an Aquahold pap pen (M-Tech, Diagnostics). The slides were placed in the humid chamber, and incubated first with Protein Block (normal goat serum [BioGenex, San Ramon, CA] diluted in PBS containing 1% bovine serum albumin, .09% sodium azide, and .1% Tween-20]), and then with primary antibodies GGH (rabbit polyclonal, gift of Dr. Thomas J. Ryan, Wadsworth Center, NY State Dept. of Health, Albany, NY; 1:1000 dilution by Universal blocking reagent [BioGenex]) and CPE (rabbit polyclonal, gift of Dr. Lloyd Fricker, Albert Einstein College of Medicine, NY; 1:500 dilution) for 1 hour. After 3 washes, the slides were incubated for 30 minutes with biotinylated goat anti-rabbit IgG (1:250 dilution; Vector Laboratories). After 3 more washes, the slides were then incubated for 45 minutes with the ABC reagent (Vector Laboratories). Slides were washed twice, placed in Tris-HCl buffer (pH 7.5) for 5 minutes, developed with liquid 3,3'-diaminobenzidine tetrahydrochloride (Dako) for 3 minutes, washed with H_2O twice, and finally counterstained lightly with Mayer's hematoxylin

for 5 seconds, dehydrated, cleared, and mounted with resinous mounting medium. Signal intensity and distribution were based on previously published methods[15,16] and scored blindly by 3 pathologists as follows: distribution score (DS) was graded as DS0, absent; DS1, <10%; DS2, 10% to 50%; DS3, 51% to 90%; or DS4, >90%. Intensity score (IS) was graded as IS0, no signal; IS1, weak; IS2, medium; or IS3, strong. The combined total score was determined as a total score (TS) = distribution (DS) + intensity (IS) (TS0, sum 0; TS1, sum 1 to 3; TS2, sum 4 to 5; TS3, sum 6 to 7). TS0 and TS1 were considered negative.

Statistics

Binomial distributions were used to compute *P* values between positive and negative immunohistochemical stains of anti-CPE or anti-GGH antibodies on tissue sections. Kaplan-Meier survival was calculated using statistical software SPSS 9.0 for Windows (SPSS, Chicago, IL). A *P* value <.05 was considered significant; <.01, very significant.

RESULTS

Microarray Analysis and Classification of Pulmonary NET

To avoid contamination with normal cells, we collected cancer cells from tissue sections by LCM (Fig 1), and used RNA extracted from these cells to conduct microarray analysis of gene expression. LCM was performed on 15 to 18 frozen sections per sample to maximize the number of cancer cells from each of 17 available fresh-frozen pulmonary NE tumor cases. High-quality total RNA (>1 μg per sample) was purified from these cells and subjected to 2 rounds of RNA amplification by T7 RNA polymerase and microarray analysis.

cDNA microarrays featuring 9984 transcripts were hybridized with probes containing Cy3-labeled cDNA from tumor RNA and Cy5-labeled reference cDNA from bronchial epithelial cell line BEAS-2B. Hierarchical clustering of the expression for 8987 transcripts (which remained after adjusting for missing values), without previous knowledge of sample identity as unsupervised analysis, revealed sample clusters that precisely matched histological classification (Fig 2).The sample containing features of SCLC and LCNEC (estimated as 90% and 10%, respectively), clustered between SCLC and LCNEC, with a shorter distance to SCLC.

We used the class comparison within BRB array tools to compare fold expression of genes in each of 3 histologically predefined groups and possibly identify genes that best discriminate among them. Based on the criterion of at least a 2-fold change and a *P* value <.004, this "supervised" analysis identified 198 genes (Table 1) that clustered all 17 tumors into 3 groups in complete agreement with their morphological classification (Fig 3).In this case, the sample with mixed features of SCLC and LCNEC again clustered with SCLC.

Our analysis revealed decreased expression of many genes, consistent with reports that the inactivation of oncogenes by deletions and chromosomal loss are associated with the development of carcinoid tu-

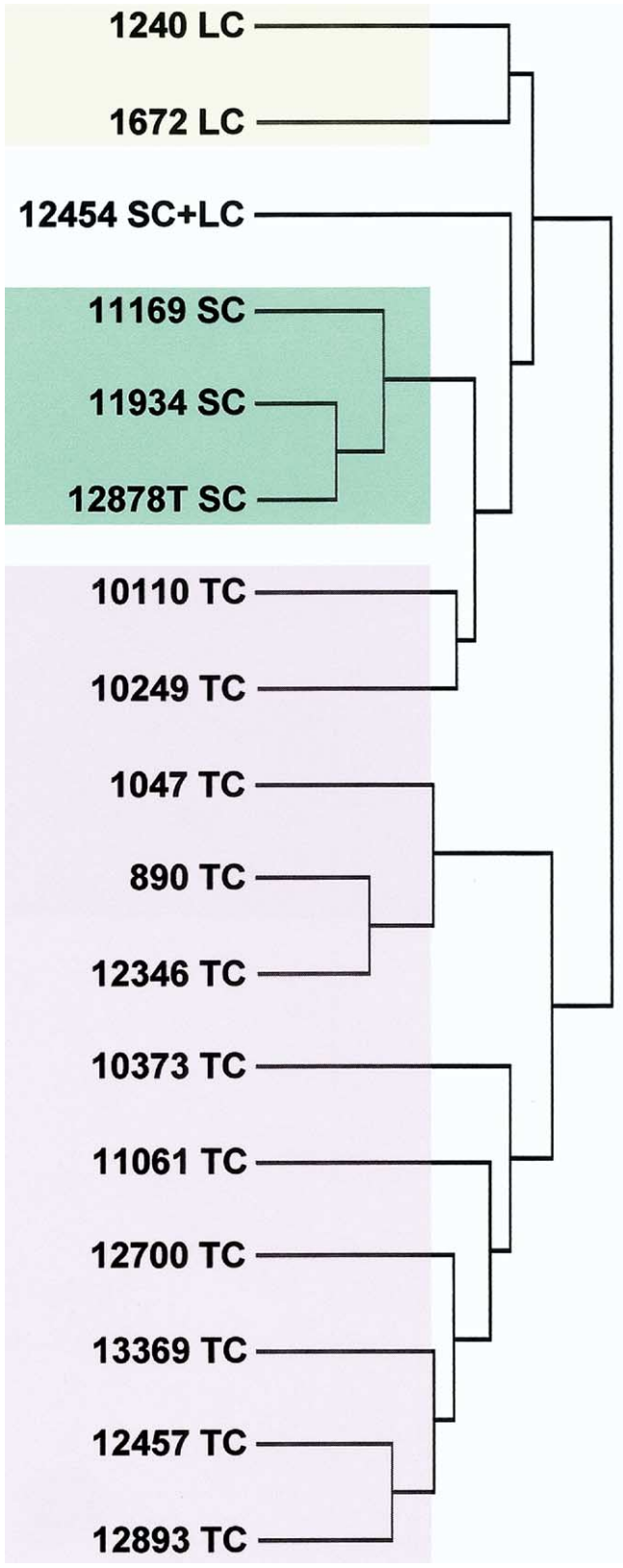

FIGURE 2. Dendogram for clustering experiments, using unsupervised data by uncentered correlation and average linkage.

TABLE 1. Cluster Genes, Using Average Linkage and Euclidean Distance, and Cutting Tree at Three Clusters

No.	Cluster	Unique ID	Gene Symbol	Map	Clone	UG Cluster
1	Cluster #1:	166807	GRIA2	4q32-q33	IncytePD:1505977	Hs.89582
2		159877	CPE	4q32.3	IncytePD:2153373	Hs.75360
3		161598	ORC4L	2q22-q23	IncytePD:2728840	Hs.55055
4		167158	C5	9q32-q34	IncytePD:1712663	Hs.1281
5	Cluster #2:	167153	GGH	8q12.1	IncytePD:1997967	Hs.78619
6		160605	P311	5q21.3	IncytePD:1555545	Hs.142827
7		169429	NR3C1	5q31	IncytePD:629077	Hs.75772
8		165192	SYNJ2	6q25-26	IncytePD:3954785	Hs.61289
9		165784	ADD3	10q24.2-q24.3	IncytePD:1481225	Hs.324470
10		163031	KIAA0751	8q23.1	IncytePD:2369544	Hs.153610
11		166328	PSMC6	12q15	IncytePD:1488021	Hs.79357
12		168061	FTHFD	3q21.3	IncytePD:2104145	Hs.9520
13		168141	DGKG	3q27-q28	IncytePD:2568547	Hs.89462
14		165076	SMG1	16p12.3	IncytePD:4253663	Hs.110613
15		167103	TAF2	8q24.12	IncytePD:998069	Hs.122752
16		169391	EIF2S1	14q23.3	IncytePD:1224219	Hs.151777
17		166789	ZNF202	11q23.3	IncytePD:1997937	Hs.9443
18		167316	SLC24A1	15q22	IncytePD:2200079	Hs.173092
19		168700	FPRL1	19q13.3-q13.4	IncytePD:523635	Hs.99855
20		165576	IL6ST	5q11	IncytePD:2172334	Hs.82065
21		168276	ITGBL1	13q33	IncytePD:1258790	Hs.82582
22		169180	IL8RB	2q35	IncytePD:561992	Hs.846
23		160957	PRKAA2	1p31	IncytePD:2507648	Hs.2329
24		160617	CSF2RB	22q13.1	IncytePD:1561352	Hs.285401
25		160429	PTK6	20q13.3	IncytePD:3255437	Hs.51133
26		160237	NPAT	11q22-q23	IncytePD:2308525	Hs.89385
27		167125	TNFRSF6	10q24.1	IncytePD:2205246	Hs.82359
28		164652	PDGFRB	5q31-q32	IncytePD:1821971	Hs.76144
29		161117	ABCG2	4q22	IncytePD:1501080	Hs.194720
30		161896	COL15A1	9q21-q22	IncytePD:4287342	Hs.83164
31		159813	PTPN12	7q11.23	IncytePD:1382374	Hs.62
32		164573	DMTF1	7q21	IncytePD:1637517	Hs.5671
33		169384	SLC22A1LS	11p15.5	IncytePD:3842669	Hs.300076
34		165393			IncytePD:3202075	Hs.351699
35		168169	OXCT	5p13	IncytePD:1685342	Hs.177584
36		165617	PRLR	5p14-p13	IncytePD:3427560	Hs.1906
37		169432	IL13RA2	Xq13.1-q28	IncytePD:3360476	Hs.25954
38		166812	MPZL1	1q23.2	IncytePD:2057323	Hs.287832
39		168428	RUNX3	1p36	IncytePD:885297	Hs.170019
40		167180	S100A4	1q21	IncytePD:1222317	Hs.81256
41		161533	CSTF2	Xq21.33	IncytePD:4016254	Hs.693
42		165588	SNAPC4	9q34.3	IncytePD:2224902	Hs.113265
43		164799	EMP3	19q13.3	IncytePD:780992	Hs.9999
44		161709	FLJ11560	9p12	IncytePD:1990361	Hs.301696
45		164868	GBP2	1pter-p13.2	IncytePD:1610993	Hs.171862
46		160233	DYRK3	1q32	IncytePD:614679	Hs.38018
47		165400	MY040	7q35-q36	IncytePD:2048144	Hs.124854
48		165957	PNLIPRP2	10q26.12	IncytePD:885032	Hs.143113
49		160054	SEC4L	17q25.3	IncytePD:1824556	Hs.302498
50		162475	CTAG2	Xq28	IncytePD:849425	Hs.87225
51		169182	LOC56311	7q31	IncytePD:2013272	Hs.73073
52		162912	DKFZP566B084	3q13	IncytePD:2680168	Hs.21201
53		163475	FLJ20485	7q22.1	IncytePD:2299818	Hs.98806
54		164927	HNRPA0	5q31	IncytePD:637639	Hs.77492
55		160630	HOXD9	2q31-q37	IncytePD:2956581	Hs.236646
56		160367	JUN	1p32-p31	IncytePD:1969563	Hs.78465
57		163762		17	IncytePD:1743234	Hs.120854
58		162247	VLGR1	5q13	IncytePD:942207	Hs.153692
59		167219	PUM1	1p35.2	IncytePD:3333130	Hs.153834
60	Cluster #3:	165171	KRT18	12q13	IncytePD:1435374	Hs.65114
61		165052	CDC20	9q13-q21	IncytePD:2469592	Hs.82906
62		167948	PIM1	6p21.2	IncytePD:2679117	Hs.81170
63		161954	ATP6F	1p32.3	IncytePD:5017148	Hs.7476
64		162391	POLE3	9q33	IncytePD:961082	Hs.108112
65		166635	KRT5	12q12-q13	IncytePD:3432534	Hs.195850
66		160035	FEN1	11q12	IncytePD:2050085	Hs.4756
67		161774	SIP2-28	15q25.3-q26	IncytePD:4626895	Hs.10803
68		162207	VAT1	17q21	IncytePD:2060308	Hs.157236
69		161163	GUK1	1q32-q41	IncytePD:2506427	Hs.3764

TABLE 1. (*Continued*)

No.	Cluster	Unique ID	Gene Symbol	Map	Clone	UG Cluster
70		161223	SIVA	22	IncytePD:2356635	Hs.112058
71		161211	CAPG	2cen-q24	IncytePD:2508570	Hs.82422
72		161948	CLDN11	3q26.2-q26.3	IncytePD:4144001	Hs.31595
73		161391	IL17F	6p12	IncytePD:1610083	Hs.272295
74		162571	PFKL	21q22.3	IncytePD:885601	Hs.155455
75		164504	CTSC	11q14.1-q14.3	IncytePD:1822716	Hs.10029
76		160565	ACY1	3p21.1	IncytePD:1812955	Hs.334707
77		169551	GSK3B	3q13.3	IncytePD:2057908	Hs.78802
78		166914	METTL1	12q13	IncytePD:1603584	Hs.42957
79		167738	CYP27B1	12q13.1-q13.3	IncytePD:1749727	Hs.199270
80		160938	HMGE	4p16	IncytePD:2074154	Hs.151903
81		162734	WNT7A	3p25	IncytePD:2622566	Hs.72290
82		165813	CASP4	11q22.2-q22.3	IncytePD:2304121	Hs.74122
83		159898	PTTG1	5q35.1	IncytePD:1748705	Hs.252587
84		161244	ARF4L	17q12-q21	IncytePD:2852403	Hs.183153
85		160715	CDC34	19p13.3	IncytePD:1857493	Hs.76932
86		163787	PYCR1	17q24	IncytePD:1702266	Hs.79217
87		160127	PGAM1	10q25.3	IncytePD:3032691	Hs.181013
88		160323	ATIC	2q35	IncytePD:2056149	Hs.90280
89		164850	IRAK1	Xq28	IncytePD:1872067	Hs.182018
90		165583	DHCR7	11q13.2-q13.5	IncytePD:3518380	Hs.11806
91		165039	TK1	17q23.2-q25.3	IncytePD:2055926	Hs.105097
92		167964	CDKN2A	9p21	IncytePD:2740235	Hs.1174
93		167223	GNB1	1p36.21-36.33	IncytePD:3562795	Hs.215595
94		167931	CSTF1	20q13.2	IncytePD:1635008	Hs.172865
95		163690	HXB	9q33	IncytePD:1453450	Hs.289114
96		161955	CNTN2	1q32.1	IncytePD:4014715	Hs.2998
97		160275	SSRP1	11q12	IncytePD:2055773	Hs.79162
98		168110	TAF12	1p35.1	IncytePD:1297269	Hs.82037
99		160102	ERP70	10	IncytePD:1824957	Hs.93659
100		167116	NP	14q13.1	IncytePD:2453436	Hs.75514
101		160802	PHB	17q21	IncytePD:1625169	Hs.75323
102		161643	ARL7	2q37.2	IncytePD:3115514	Hs.111554
103		162343	LIMK2	22q12.2	IncytePD:958513	Hs.278027
104		162727	PTK9L	3p21.1	IncytePD:3999291	Hs.6780
105		160262	DDX28	16q22.1	IncytePD:2663948	Hs.155049
106		165790	SURF1	9q33-q34	IncytePD:1921567	Hs.3196
107		168638	HDAC7A	12q13.1	IncytePD:1968721	Hs.275438
108		168079	EMP1	12p12.3	IncytePD:1624024	Hs.79368
109		160999	P114-RHO-GEF	19p13.3	IncytePD:1734113	Hs.6150
110		161790	KIAA0469	1p36.23	IncytePD:2674277	Hs.7764
111		169691	E2-EPF	17p12-p11	IncytePD:2057823	Hs.174070
112		163682	DPH2L2	1p34	IncytePD:1810821	Hs.324830
113		168266	PSME3	17q12-q21	IncytePD:1308112	Hs.152978
114		161374	POLA2	11q13.1	IncytePD:3179113	Hs.81942
115		164646	GALE	1p36-p35	IncytePD:1807294	Hs.76057
116		162150	APOL1	22q13.1	IncytePD:2056987	Hs.114309
117		164206	FN14	16p13.3	IncytePD:1402615	Hs.10086
118		162623	BAK1	6p21.3	IncytePD:2055687	Hs.93213
119		162244	ARHGDIA	17q25.3	IncytePD:2055640	Hs.159161
120		164586	ITPA	20p	IncytePD:1931265	Hs.6817
121		165483	PDAP1	7q22.1	IncytePD:3032825	Hs.278426
122		166195	APRT	16q24	IncytePD:2751387	Hs.28914
123		166960	APG12L	5q21-q22	IncytePD:2058537	Hs.264482
124		167505	TST	22q13.1	IncytePD:1988239	Hs.351863
125		168642	ST14	11q24-q25	IncytePD:478960	Hs.56937
126		167170	DXS1283E	Xp22.3	IncytePD:1567995	Hs.264
127		161754	ACTG2	2p13.1	IncytePD:3381870	Hs.78045
128		166010	RIPK1	6p25.3	IncytePD:2180031	Hs.296327
129		161794	SCAMP2	15q23-q25	IncytePD:3123858	Hs.238030
130		167591	COMT	22q11.21	IncytePD:605019	Hs.240013
131		162587	POLR2D	2q21	IncytePD:696002	Hs.194638
132		169071	CAPZB	1p36.1	IncytePD:1853163	Hs.333417
133		160467	POLD2	7p13	IncytePD:2056172	Hs.74598
134		162178	C2F	12p13	IncytePD:5096975	Hs.12045
135		167706	GMPPB	3p21.31	IncytePD:1486983	Hs.28077
136		160803	FARSL	19p13.2	IncytePD:1808260	Hs.23111
137		169254	POLM	7p13	IncytePD:771715	Hs.46964
138		167351	MYBPH	1q32.1	IncytePD:3010959	Hs.927
139		163276		7	IncytePD:2383065	Hs.25892

TABLE 1. (*Continued*)

No.	Cluster	Unique ID	Gene Symbol	Map	Clone	UG Cluster
140		167135	ERCC1	19q13.2-q13.3	IncytePD:2054529	Hs.59544
141		160478	G5B	6p21.3	IncytePD:1942845	Hs.73527
142		162631	TADA3L	3p25.2	IncytePD:3990209	Hs.158196
143		163921	GNPI	5q21	IncytePD:1653911	Hs.278500
144		160098	MRPL49	11q13	IncytePD:1755793	Hs.75859
145		161058	MEN1	11q13	IncytePD:1693847	Hs.24297
146		160038	BAD	11q13.1	IncytePD:3967780	Hs.76366
147		162220	FKBP1A	20p13	IncytePD:4059193	Hs.349972
148		161026	HSXQ28ORF	Xq28	IncytePD:1669254	Hs.6487
149		167607	TRAP1	16p13.3	IncytePD:1960722	Hs.182366
150		167713	KIAA0175	9p11.2	IncytePD:3805046	Hs.184339
151		165648	DUSP4	8p12-p11	IncytePD:740878	Hs.2359
152		161574	FRAT2	10q23-q24.1	IncytePD:3871545	Hs.140720
153		161650	KIAA0415	7p22.2	IncytePD:2798872	Hs.229950
154		168386	NOLC1	10	IncytePD:1431819	Hs.75337
155		159906	H2AFX	11q23.2-q23.3	IncytePD:1704168	Hs.147097
156		167906	RAE1	20q13.31	IncytePD:2914719	Hs.196209
157		160486	DTX2	7q11.23	IncytePD:1691161	Hs.89135
158		160678	MAFG	17q25	IncytePD:2956906	Hs.252229
159		159889	FUS	16p11.2	IncytePD:3038508	Hs.99969
160		167553	LIG1	19q13.2-q13.3	IncytePD:1841920	Hs.1770
161		163824	UNG	12q23-q24.1	IncytePD:1405652	Hs.78853
162		161012	GCN1L1	12q24.2	IncytePD:1699149	Hs.75354
163		162006	REG1B	2p12	IncytePD:2374294	Hs.4158
164		161454	SPINT1	15q13.3	IncytePD:2722572	Hs.233950
165		162510	CAMKK2	12	IncytePD:557451	Hs.108708
166		163306	BLM	15q26.1	IncytePD:2923082	Hs.36820
167		160242	RNUT1		IncytePD:1562658	Hs.21577
168		164106	GRWD	19q13.33	IncytePD:1561867	Hs.218842
169		165799	MADH3	15q21-q22	IncytePD:1858365	Hs.211578
170		166574	SNAPC2	19p13.3-p13.2	IncytePD:1445203	Hs.78403
171		160441	LTBR	12p13	IncytePD:899102	Hs.1116
172		168453	TACC3	4p16.3	IncytePD:2056642	Hs.104019
173		164244	PSMC4	19q13.11-q13.13	IncytePD:2806778	Hs.211594
174		169564	SMARCD2	17q23-q24	IncytePD:1890919	Hs.250581
175		161178	BSG	19p13.3	IncytePD:2182907	Hs.74631
176		165614	JUP	17q21	IncytePD:820580	Hs.2340
177		168987	HRMT1L2	19q13.3	IncytePD:2888814	Hs.20521
178		167987	ENTPD1	10q24	IncytePD:1672749	Hs.205353
179		163726	C3	19p13.3-p13.2	IncytePD:1513989	Hs.284394
180		164642	YARS	1p34.3	IncytePD:1559756	Hs.239307
181		160303	ERF	19q13	IncytePD:2057547	Hs.333069
182		161635	TYMSTR	3p21	IncytePD:2610374	Hs.34526
183		159859	GS2NA	14q13-q21	IncytePD:1339241	Hs.183105
184		161051	MARK3	14q32.3	IncytePD:2395018	Hs.172766
185		161835	PEX10	1p36.11-1p36.33	IncytePD:3115936	Hs.247220
186		165571	ANXA3	4q13-q22	IncytePD:1920650	Hs.1378
187		164286	NFKBIE	6p21.1	IncytePD:2748942	Hs.91640
188		165786	HYAL2	3p21.3	IncytePD:1240748	Hs.76873
189		161620	H4FE	6p22-p21.3	IncytePD:3728255	Hs.278483
190		168302	TIP-1	17p13	IncytePD:1997792	Hs.12956
191		160887	PES1	22q12.1	IncytePD:2758740	Hs.13501
192		162419	RAE1	20q13.31	IncytePD:588157	Hs.196209
193		169625	RFC4	3q27	IncytePD:1773638	Hs.35120
194		163425	TCEA2	20	IncytePD:818568	Hs.80598
195		166359	TUBB	6p21.3	IncytePD:3334367	Hs.336780
196		161947	TIM17B	Xp11.23	IncytePD:1727491	Hs.19105
197		162236	KIAA0670	14q11.1	IncytePD:1968610	Hs.227133
198		168426	RTVP1	12q15	IncytePD:477045	Hs.64639

mors.[17] Decreased expression of genes involved in DNA synthesis and repair, such as Bloom (*BLM*), was a common feature for TC and LCNEC; whereas DNA excision repair (*ERCC1*) and DNA ligase-1 (*LIG*) were suppressed in all tumor types. Loss of expression of genes that regulate cell–cell and cell–matrix interactions was also apparent in all tumor types. Other groups of genes with decreased expression in all tumors were involved in cell cycle control (*CDC34*, p16/CDK inhibitor 2A), suppression of the MAPK pathway (dual-specificity phosphatase, *DUSP4*), and tumor suppression (epithin, *ST14*, and prohibitin, *PHB*). Increased expression of several genes associated with cell growth, such as *CSF1R*, *RTK*, and *P311* (a gene implicated in the inva-

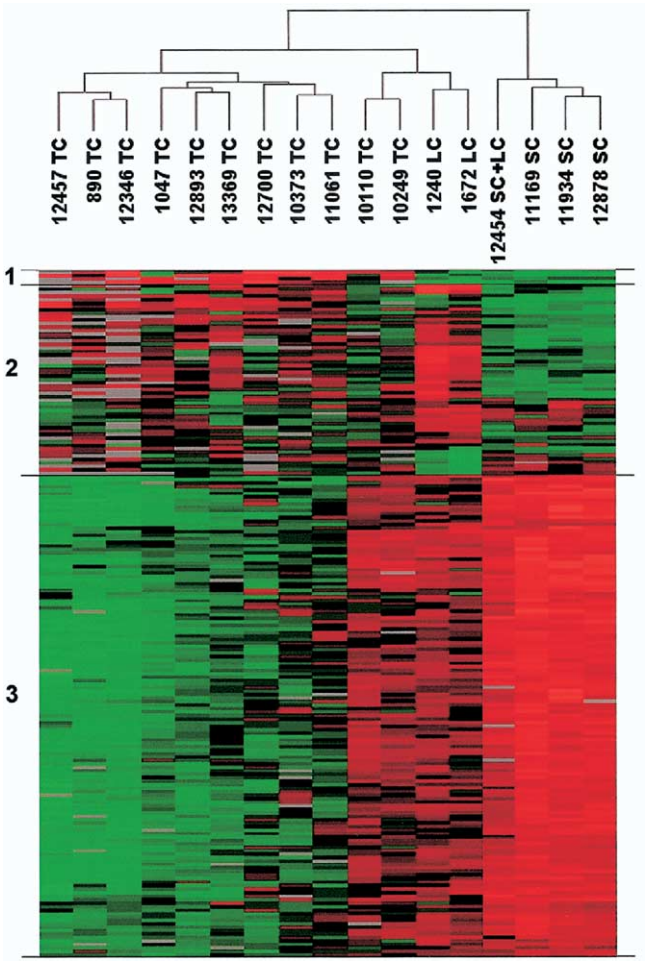

FIGURE 3. Dendrogram of pulmonary NE tumors based on expression of 198 genes. Seventeen cases of the NE tumors were sorted by 1-way hierarchical clustering based on the expression similarities of 198 genes that were selected from 9984 genes based on the expression changes in the 3 subtype tumors with significant statistical difference (*F*-test, $P < .004$). Red, green, and black signal indicate that expression of these genes is higher, lower, or equal to the median level of expression in all samples, respectively. Gray represents missing genes or poor quality data. The numbers are the case numbers of the tumor samples. The numbers 1, 2, and 3 on the left side of the color image correspond to the gene cluster numbers in Table 1.

sion of glioblastomas[18]) showed higher expression in LCNEC than in other tumors or normal lung.

The expression of anti-apoptotic genes, such as BCL2 antagonist-killer, *BAK1*, and *caspase-4*, was decreased in all 3 tumor subtypes. In addition, a >2.5-fold decrease in the BAD and tumor necrosis factor receptor-interacting kinase, RIPK1, was evident in TC and LCNEC. BAD and BAK1 are located on chromosomes 11q13 and 6p21, respectively, both of which are sites of loss of heterozygosity, as was previously reported for pulmonary NE tumors,[19,20] although a gain of chromosomal material on 6p21 detected by comparative genomic hybridization has been reported.[21] The decrease of BAK1 in TC and LCNEC was less than 2-fold, indicating that in addition to LOH, suppression of p53-mediated transcriptional activation[22] or DNA methylation[23] also may be operating in these tumors.

Selection of Candidate Genes as Biomarkers for NE tumors

We conducted 2 × 2 comparisons on relative expression ratios of 198 genes between the 3 tumor subtypes. Using the criteria that the difference in gene expression in 1 tumor subtype must be at least 2.5-fold greater than in the other 2, we identified 48 genes that distinguished each tumor subtype from the others. There were 5 genes in TC, 7 in LCNEC, and 36 in SCLC that fulfilled such criteria. Table 2 lists expression ratios of the 48 classifier genes along with major function, chromosomal location, previous reports of changes identified by LOH or GGH, and UniGene cluster number.

Validation of Gene Expression by Real-Time Quantitative RT-PCR

To validate changes in expression among 48 classifier genes, we performed quantitative real-time RT-PCR (qRT-PCR) analysis on several genes selected from each group, based on high expression ratio and availability of antibodies for further validation by immunohistochemistry. These genes were CPE, complement component 5 (C5), P311 protein (P311), GGH, cell division cycle 20 (CDC20), and cell division cycle 34 (CDC34). Expression changes of each gene were normalized to 18S RNA in each sample and compared with the expression level in the reference RNA from the BEAS-2B cell line. The results show that relative expression changes were generally consistent with microarray results (Fig 4).

CPE and GGH Protein Expression in Different Subtypes of pulmonary NE Tumors

To determine protein expression in archived pulmonary NE tumor tissue sections, we tested antibodies to protein products of the same genes used for qRT-PCR. Antibodies that recognize 2 gene products, CPE and GGH, were technically suitable for immunohistochemistry on all tissue samples. These antibodies were used to detect CPE and GGH protein levels on a total of 68 available pulmonary NE tumors, and generated informative data on 55 cases. IHC slides were reviewed and scored independently by 3 pathologists; the final scores represent consensus from their individual readings. Figure 5A shows one representative image stained by anti-CPE antibody of tissue sections of normal lung, TC, LCNEC, and SCLC. No signal is detected in normal bronchial epithelial cells or pneumocytes. Some staining appeared in scattered NE cells of terminal bronchiolar epithelia and macrophages. The TC sample showed a strongly positive stain with uniform signal in the cytoplasm and the cell membrane. The LCNEC section had a weak and scattered anti-CPE staining, whereas SCLC was negative. Figure 5B shows images obtained using anti-GGH antibody. Normal lung tissue and the TC section demonstrated no detectable signal. LCNEC and SCLC samples were positive. Most staining was

TABLE 2. Expression Ratios of 48 Classifier Genes Between TC, LCNEC (LC), and SCLC (SC)

No.	Gene Symbol	Relative Expression		Function	Map	Cytogenetic Alterations by LOH and GGH[19,33,34]	UniGene Cluster
		TC/SC	TC/LC				
1	C5	5.6	7.5	Immune	9q32-q34	Loss, SCLC; gain LCNEC	Hs.1281
2	CPE	6.3	4.2	Biosynthesis	4q32.3	Loss, SCLC	Hs.75360
3	GRIA2	5.5	4.0	Receptor	4q32-q33	Loss, SCLS & LCNEC	Hs.89582
4	RIMS2	3.1	2.6	Synaptic exocytosis	8q23.1		Hs.153610
5	ORC4L	2.7	3.2	DNA replication	2q22-q23	YesLoss, SCLC & LCNEC	Hs.55055
		LC/TC	LC/SC				
1	CSF2RB	3.8	4.2	Receptor	22q13.1	Loss, SCLC; gain LCNEC	Hs.285401
2	GGH	4.8	6.3	Drug resistance	8q12.1	Gain, LCNEC	Hs.78619
3	NPAT	2.5	3.8	Cell cycle	11q22-q23	Loss, SCLC	Hs.89385
4	NR3C1	3.8	5.7	Transcription factor	5q31	Loss, SCLC & LCNEC	Hs.75772
5	P311	5.6	7.1	Focal adhesion	5q22.2	Gain or loss, SCLC; loss, LCNEC	Hs.413760
6	PRKAA2	2.8	4.2	Metabolism	1p31	Gain, SCLC	Hs.2329
7	PTK6	2.7	3.6	Oncogene	20q13.3	Gain, SCLC & LCNEC	Hs.51133
		SC/TC	SC/LC				
1	APRT	5.1	2.9	Metabolism	16q24	Loss, SCLC	Hs.28914
2	ARF4L	5.4	3.8	Protein secretion	17q12-q21	Gain, SCLC	Hs.183153
3	ARHGDIA	3.7	2.5	RAS gene family	17q25.3	Gain, SCLC & LCNEC	Hs.159161
4	ARL7	4.8	3.0	Endocytosis	2q37.2		Hs.111554
5	ATP6F	4.1	3.3	Proton transport	1p32.3	Gain, SCLC	Hs.7476
6	CDC20	7.5	3.3	Cell cycle, G1	1p34.1	Loss, SCLC	Hs.82906
7	CDC34	5.5	2.8	Cell cycle, G2	19p13.3	Gain, SCLC	Hs.423615
8	CLDN11	6.2	2.9	Tight junction	3q26.2-q26.3	Gain, SCLC; loss LCNEC	Hs.31595
9	COMT	3.3	2.6	Neurotransmission	22q11.21	Gain, LCNEC	Hs.240013
10	CSTF1	2.8	2.6	Polyadenylation	20q13.2	Gain, SCLC	Hs.172865
11	DDX28	4.8	3.1	RNA helicase	16q22.1	Loss, SCLC	Hs.155049
12	DHCR7	5.6	2.8	Metabolism	11q12-q13	Gain, SCLC	Hs.11806
13	ERP70	4.7	2.7	Metabolism	7q35		Hs.93659
14	FEN1	6.5	3.4	Endonuclease	11q12	Gain, SCLC, loss TC & AC	Hs.4756
15	GCNIL1	3.7	2.6	Translation	12q24.2		Hs.75354
16	GNB1	3.3	2.9	Signal transduction	1p36.33	Gain, SCLC & LCNEC	Hs.215595
17	GUK1	6.6	2.9	Signal transduction	1q32-q41	Gain, SCLC	Hs.3764
18	HDAC7A	4.1	2.8	Cell cycle, chromatin	12q13.1		Hs.275438
19	ITPA	4.8	2.8	Metabolism	20p	Loss, SCLC; gain, LCNEC	Hs.6817
20	JUP	4.1	2.6	Cell adhesion	17q21	Gain, SCLC, LCNEC & TC	Hs.2340
21	KIAA0469	4.5	2.8		1p36.23		Hs.7764
22	KRT5	5.7	3.5	Intermediate filaments	12q12-q13		Hs.433845
23	PDAP1	4.3	3.0	Growth factor	7q22.1	Gain, SCLC	Hs.278426
24	PGAMI	4.4	3.1	Metabolism	10q25.3	Loss, SCLC & LCNEC	Hs.181013
25	PHB	4.9	2.8	Antiproliferation	17q21	Gain, SCLC & LCNEC	Hs.75323
26	POLA2	4.7	2.6	RNA synthesis	11q13.1	Gain, SCLC	Hs.81942
27	POLD2	3.7	2.6	DNA replication	7p13	Loss, SCLC	Hs.74598
28	POLE3	5.5	3.5	Histone-fold	9q33	Gain, LCNEC	Hs.108112
29	PYCR1	4.5	2.6	Metabolism	17q24	Gain, SCLC & LCNEC	Hs.79217
30	SIP2-28	5.2	2.9	Receptor	15q25.3-q26	Loss, SCLC	Hs.10803
31	SIVA	6.5	3.6	Apoptosis	14q32.33		Hs.112058
32	SURF1	3.8	2.5	Neurologic disorder	9q33-q34	Gain, LCNEC	Hs.423854
33	TADA3L	2.8	2.5	P53 cofactor	3p25.2	Loss, SCLC & LCNEC	Hs.158196
34	TK1	4.8	2.7	Metabolism	17q25.2-q25.3	Gain, SCLC	Hs.105097
35	TYMSTR	3.0	2.5	Signal transduction	3p21	Loss, SCLC	Hs.34526
36	VATI	4.5	3.4	Neurotransmission	17q21	Gain, SCLC	Hs.157236

FIGURE 4. Comparisons of expression changes detected by real-time RT-PCR and microarrays. RNA isolated from LCM cells was examined in triplicate for expression changes of 6 genes in the 17 pulmonary NET specimens. Relative expression changes of 6 genes detected by qRT-PCR (left panels) were presented here in comparisons with those derived from cDNA microarray analysis (right panels). The expression of each gene in qRT-PCR analysis was normalized, first by the expression of the 18S ribosomal gene in the same cell line, and then by the expression of that gene in the BEAS-2B control cells. The 17 pulmonary NET cases were arranged from left to right in each panel in the same order of 1240, 1672, 11169, 11934, 12454, 12878, 890, 1047, 11061, 12346, 12457, 12893, 13369, 10110, 10249, 10373, and 12700. The primer pairs (probes) for qRT-PCR are as follows:CPE: 5'-TTGTCCGAGACC TTCAAGGTAAC-3' and 5'- CCTTTGCGGATG-TAACATCGT-3' (5'-TTGCGAATG CCACCATCTCCGTG-3')C5: 5'-GATTCCGGATATTTGAACTCTTTGA-3' and 5'-TATTGGAAGTGCTATA-AAACATGGTACA-3' (5'-TTG GGTTTCTCAGTCCTGCCACTTTCA-3')P311: 5'-CTGGGTCAGTCAAGAACCATTTC-3' and 5'-ACTTCCTTT-GGGACAGGAAGTCT-3' (5'-TTAGGA AGCCTTCCCTCCATGTCCTTGTTT-3')GGH: 5'-GAGTTTATTTCAACAATGGAAGGATATAAG-3' and 5'-TGGGAAATGCCATCCAAATT-3' (5'- CTG GATGCCACTGGACACCATATACTGGAT-3')CDC20: 5'-CTGAACGGTTTTGATGTA-GAGGAA-3' and 5'-CCCTCTGGCGCATTTTGT-3' (5'-CCAAGATCC TTCGGCTCAGTGGAAAAC-3')CDC34: 5'-TTCTCGCCCG-CAAACGT-3' and 5'-ACCTGCTTCCGGATGATGTCT-3' (5'-TCCACTTCCTGTACA TCACGGAGGCG-3')

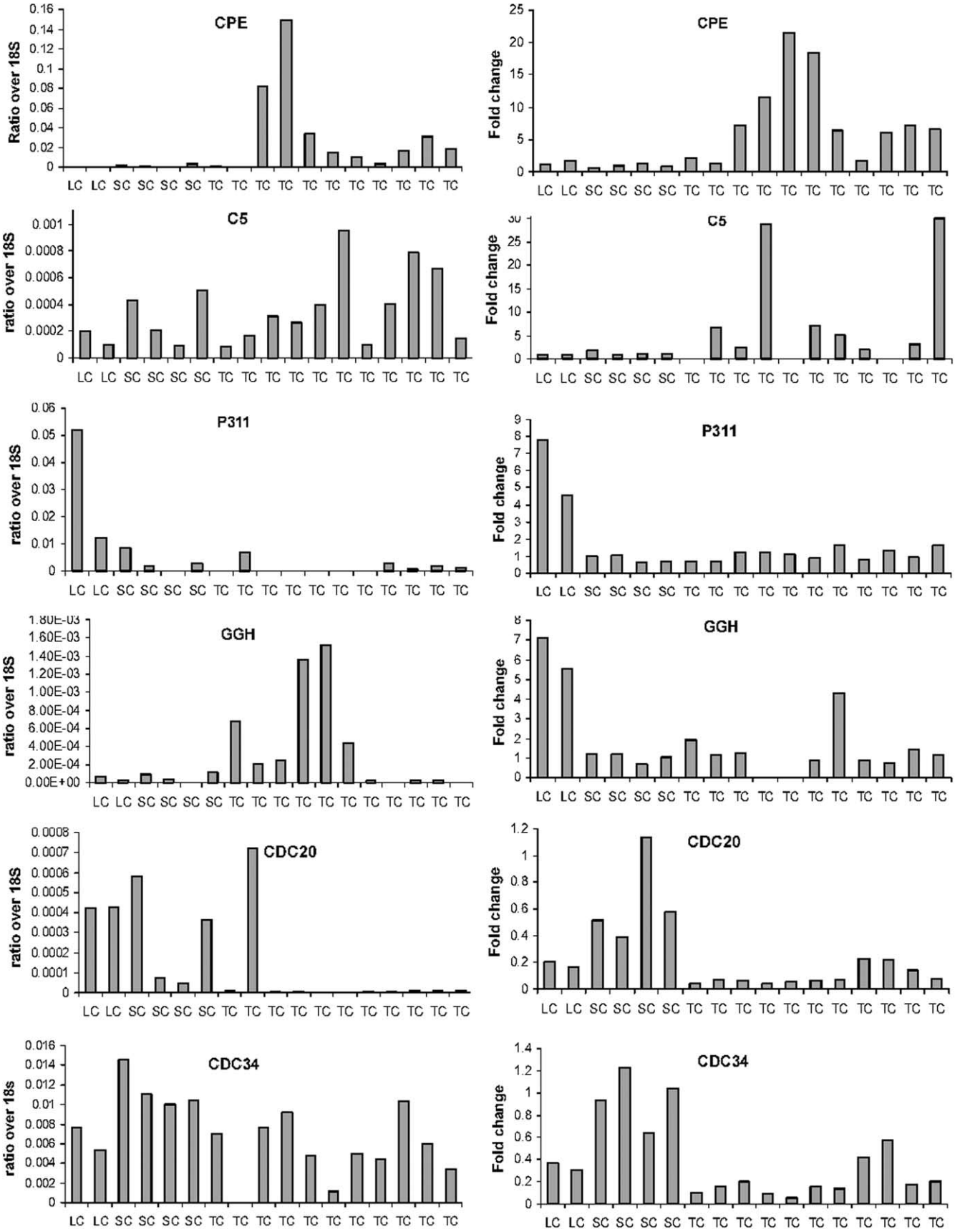
CPE
Ratio over 18S
Fold change
C5
ratio over 18S
Fold change
P311
ratio over 18S
Fold change
GGH
ratio over 18S
Fold change
CDC20
ratio over 18S
Fold change
CDC34
ratio over 18s
Fold change
LC LC SC SC SC SC TC TC TC TC TC TC TC TC TC TC

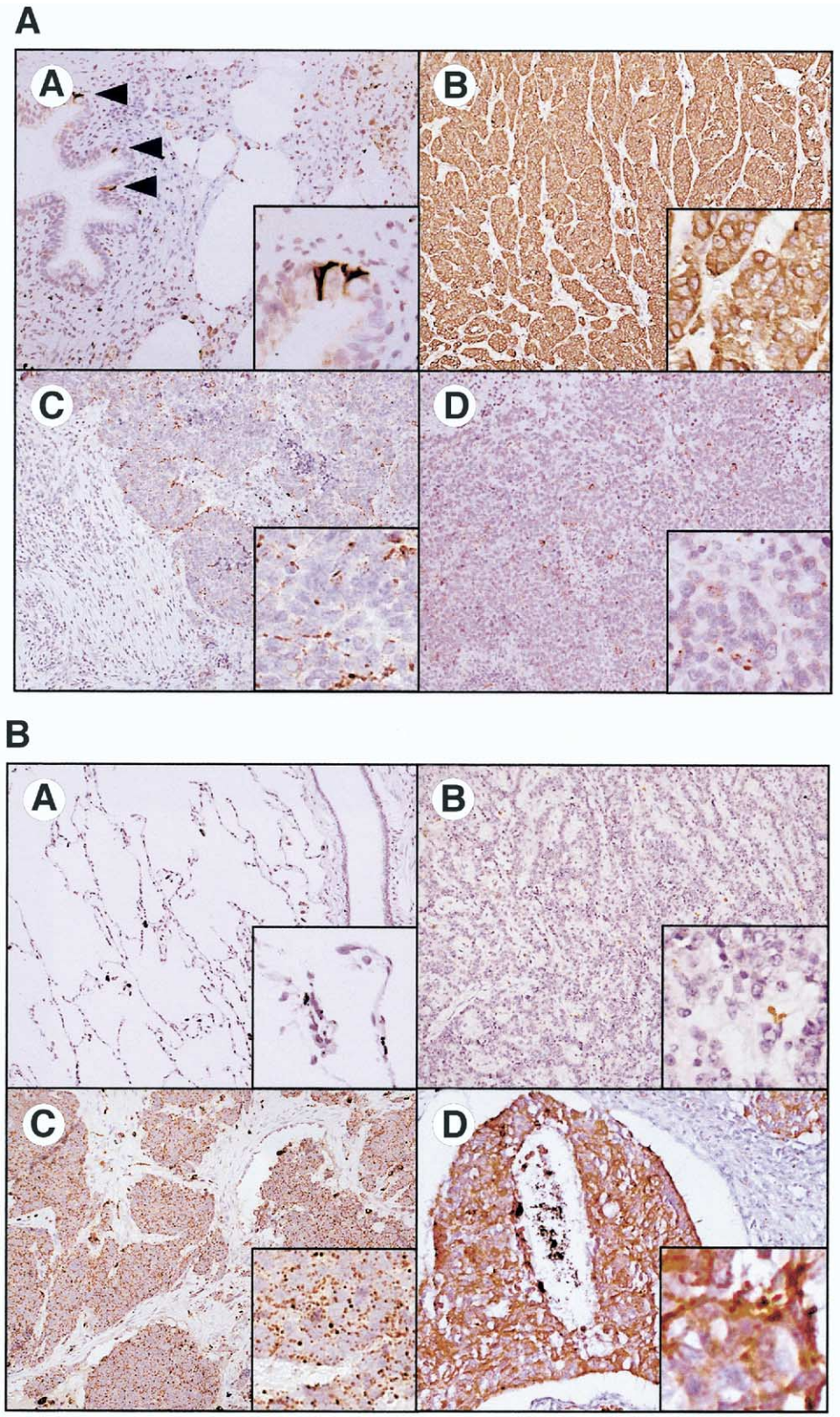

FIGURE 5. IHC-stained images. IHC, using anti-CPE and anti-GGH antibodies, was performed on 17 pulmonary NE tumors used in microarray gene expression analysis and an additional 51 pulmonary NE tumors for cross-validation of the CPE and GGH protein expression. (A) Anti-CPE stain. (a) Normal lung, negative. No signals are in bronchial epithelia or pneumocytes. Strong staining appears only in scattered NE cells in terminal bronchiolar epithelia (arrowheads). (b). TC, strong positive signals. Intense and uniform membranous and cytoplasmic stain is seen in all tumor cells. (c) LCNEC, negative, and (d) SCLC, negative. Only occasional tumor cells exhibit weak intracytoplasmic staining. (B) Anti-GGH stain. (a) Normal lung, negative. (b) TC, negative. The tumor cells have no detectable signals, and mild staining can be seen only in scattered stromal cells. (c) LCNEC, positive. All tumor cells show intracytoplasmic staining with course granular pattern. (d) SCLC, positive intracytoplasmic staining in all tumor cells.

TABLE 3. Immunohistochemistry on 55 Pulmonary NE Tumors

Pulmonary NE Tumor	Anti-CPE			Anti-GGH		
	Positive	Negative	*P* value*	Positive	Negative	*P* value
TC	16	5	.017	7	14	.189
AC	4	1	.625	0	5	.063
LCNEC	1	7	.070	8	0	.008
SCLC	4	17	.007	16	5	.017
Total	23	32		31	24	

**P* value refers to the difference between the percent of positive and negative samples within each type of pulmonary NE tumors, as calculated by *t*-test.

cytoplasmic with a course granular pattern. No nuclear signal was detected. Table 3 summarizes the results of anti-CPE and anti-GGH staining from all 55 samples.

Statistical analysis was based on binomial distribution of positive and negative results. *P* values were calculated using the Student *t*-test for the percentage of positive samples in each tumor type. Of 21 cases of TC, 16 (76%) were positive for CPE and 5 (24%) were negative. This difference is statistically significant, with $P = .017$. The anti-GGH stain on 21 cases of TC was positive in 7 (33%) and negative in 14 (67%). Four of 5 (80%) AC cases were positive for anti-CPE, and all 5 AC cases were negative for GGH (100%). Staining for CPE was negative in 7 of 8 samples with LCNEC (88%), but all 8 of these samples (100%) were positive for GGH. <Of 21 cases of SCLC, only 4 (19%) were positive for CPE, and 16 (76%) were positive for GGH. These differences in SCLC expression are also statistically significant, with $P = .007$ and .017, respectively. Therefore, the CPE gene product is expressed in low- and intermediate-grade NE tumor subtypes, TC and AC, whereas GGH is expressed in high-grade NE tumors, LCNEC and SCLC.

CPE and GGH Protein Expression Predict Survival Rates of Patients With Pulmonary NE Tumors

We performed Kaplan-Meier survival analysis of positive CPE or GGH stains on all 54 patients for whom we had information on clinical outcome. The 9-year survival probability for the patients positive for CPE was 76%, which was significantly higher ($P <.02$) that that in the patients negative for CPE (27%) (Fig 6A).In contrast, the 9-year survival probability for was only 28% for patients with positive GGH staining, but was 83% in patients with negative GGH (Fig 6B). These differences are also statistically significant ($P <.01$).

DISCUSSION

Hierarchical clustering was developed to analyze gene expression data from DNA microarrays. The technique is based on statistical algorithms to arrange genes and samples according to similarities in gene expression.[14] In our study, unsupervised analysis of the cDNA gene expression profile resulted in a precise classification of pulmonary NE tumors according to their histological subtype. This is rarely achieved from the analysis of primary tumors. We consider that using a large number of cancer cells isolated by LCM, combined with nonbiased RNA amplification, contributed to the accurate classification of tumor samples by unsupervised analysis. Total RNA used for our experiments was extracted from >10,000 cancer cells dissected from at least 15 sections by LCM and subjected to 2 rounds of amplification. In a previous study, Luo et al,[13] used T7 polymerase-based amplification of RNA isolated from LCM cells for accurate cDNA microarrays. Total RNA was extracted from 1000 neuronal cells and subjected to 3 rounds of amplification before microarray analysis. Correlation of signal intensities between the same sam-

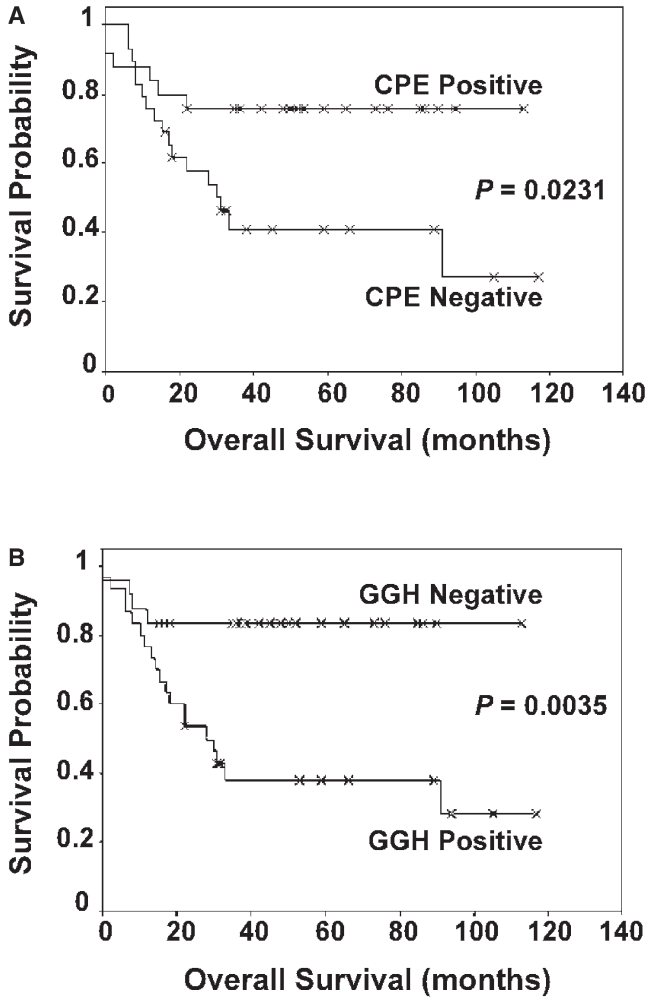

FIGURE 6. Kaplan-Meier survival rates of 54 cases of pulmonary NET patients as function of CPE or GGH expression. (A) Survival rates of patients with positive and negative CPE stains on pulmonary NET cells. The survival rate (76%) for the patients with the positive CPE is statistically significant ($P = .023$), higher than that (27%) with the negative stain. (B) Inverse correlation of survival rates to the GGH expression in pulmonary NET cells. The survival rates for positive and negative GGH stains in pulmonary NET cells were 28% and 83%, respectively, with the statistic significance ($P = .0035$). X indicates censored samples.

ples varied from 93% to 97%. In addition, Xiang et al[24] have reported that RNA can be amplified reliably from as few as 10 cells using as many as 4 rounds of amplification, whereas we used only 2 amplification rounds.

A class comparison test using BRB array tools led to the identification of 198 from 9984 genes (1.98%), with statistical significance ($P < .004$) and accurate classification of histologically predetermined tumor subtypes. A 2 × 2 comparison of the 198 genes between the 3 subtypes of pulmonary NE tumors identified 48 candidate genes that distinguished each tumor subtype from the other 2 subtypes.

The purpose of the present study was not to generate a definitive algorithm for the classification of pulmonary NE tumors, but rather to identify an expression profile that distinguishes each tumor subtype and tumor-specific biomarkers. Because the sample size of some subtypes of NE tumors was too small to permit full statistical analysis by class prediction, the clustering of selected genes needs to be validated by a larger set of tumors that should also include samples from patients with AC.

Comparative analysis of tumor samples with immortalized bronchoepithelial cells, believed to be the cell of origin for these tumors, may have also contributed to the accurate classification of these tumors. It is often difficult to obtain reference RNA for studying human primary tumors. To date, most studies use samples pooled from normal tissue or a portion of each test sample as a reference. In a previous microarray study from our laboratory,[8] RNA isolated from BEAS-2B was used as the reference for microarray-based classification of non–small cell lung cancer samples, resulting in a reliable expression profile. Here BEAS-2B cells were again successfully used as a reference for the classification of pulmonary NE tumors. Although genetic alterations can occur during consecutive passage of immortalized cells in culture, we used RNA from early-passage BEAS-2B cells, which have minimal chromosomal alterations.[25] The results of our study indicate that accurate classification of tumors can be achieved by comparing gene expression profiles in the tumors with normal cells derived from the same organ. Whether RNA from BEAS-2B cell can be used for the analysis of gene expression in NE tumors from other organs or whether this method is applicable to tumors from other organs, such as the brain, where availability of normal tissue is limited, remains to be established.

Changes in the expression of several genes identified in the present study may have implications for ongoing trials using molecular targeted therapies. Decreased expression of genes associated with the ubiquitin pathway, such as the proteasome subunit 26S (*PSMC4*) and proteasome activator subunit 3 (*PSME3*), could contribute to the activation of NFkB and may influence the response to proteasome inhibitors. We also found the suppression of several antagonists of BCL2, such as BAK1, caspase-4, BAD, and the tumor necrosis factor receptor-interacting kinase, RIPK1. The suppression of BAX, another antagonist of BCL2, has been also described in SCLC.[22] The overexpression of BCL2 has not been previously detected in pulmonary NE tumors and was not evident in our study. However, our results indicate that pulmonary NE tumors lack several pro-apoptotic genes that antagonize BCL2. This is in contrast with the overexpression of BCL2, which is implicated in survival and drug resistance of other tumors.[26] It is possible that targeting the BCL2 pathway for therapy in drug-sensitive but almost uniformly relapsing tumors, such as SCLC, can improve their outcome. This will soon be apparent from results of currently ongoing clinical trials using antisense oligonucleotide to BCL2 and BCL-xL.

Other investigators have reported gene expression profiles, using lung cancer specimens on different microarray platforms, including some pulmonary NE tumors,[7,9,10] and have provided datasets with complex combinations of genes for SCLC and carcinoid tumors. Unfortunately, this information cannot be reliably compared with the present study, because different gene chips and controls were used, but several genes presented here (including *CPE*, *P311*, and others) have been previously reported by other investigators. This further supports the results presented here. Microarray analysis of 203 lung cancer samples, including 20 carcinoids and 6 SCLCs, was performed by Bhattacharjee et al,[7] who reported that 1 gene in a small group of genes, distinguished NE tumors from all other lung cancers—*CPE*, a gene found to be overexpressed in well-differentiated carcinoid tumors in our study.

We internally validated the expression of *CPE* by qPCR in tumors analyzed by microarray, and cross-validated the expression of CPE gene product on additional cases of NE tumors by IHC. CPE is a secreted neuropeptide-processing enzyme expressed primarily in the brain, cells of NE origin in various organs, and prostatic stromal cells. CPE exists in membrane-bound and soluble forms in normal tissues.[27] We found that the CPE protein accumulated in cytoplasmic and membrane-associated forms in well-differentiated carcinoids. CPE is located on chromosome 4p33, which is rarely deleted in lung cancers. A mutant mouse with the deletion of CPE is obese and has an altered metabolism due to improper secretion, folding, and degradation of prohormones, secretins, and neuropeptides.[28] Thus the overexpression of CPE may contribute to elevated levels of many neuropeptides, a feature frequently observed in patients with carcinoid tumors. Whether or not CPE is expressed in other carcinoid tumors, such as gastrointestinal NE tumors, remains to be established.

A second marker, identified from microarray analysis and cross-validated by immunohistochemistry, was GGH, a lysosomal enzyme that catalyzes the hydrolysis of folypoly-γ-glutamates and antifolypoly-γ-glutamates by the removal of γ-linked polyglutamates and glutamate.[29] In tumor samples, mRNA for *ggh* was increased specifically in LCNEC. This increase corresponded to protein accumulation based on IHC, indicating transcriptional activation. However, the *ggh* gene may be also regulated in tumors at posttranscriptional levels, because the anti-GGH antibody detected high levels of the GGH protein in 3 of 4 SCLC cases, whereas no

increase in mRNA was observed in these samples by microarray or qRT-PCR. Study of *ggh* transcriptional and translational regulation may be important, because it could have diagnostic and prognostic value, and also because GGH is implicated in methotrexate resistance in sarcomas[30] and leukemias.[31,32]

IHC study of 55 cases of pulmonary NE tumors confirmed that positive CPE and negative GGH are more frequent events in low-grade TC and intermediate-grade AC and, thus are good prognostic indicators. Indeed, survival analysis correlated positive CPE and negative GGH with the best prognostic outcome. In contrast, both LCNEC and SCLC tissue samples were positive for GGH. Thus, positive CPE and negative GGH correlate with good prognosis for pulmonary NET patients, whereas positive GGH and the absence of CPE suggest the opposite outcome.

This is the first report to correlate the expression of specific markers, CPE and GGH, to pulmonary NE tumor grade prognosis. Whether these markers can be used as independent variables of survival remains to be established.

Acknowledgment. We thank Amy Peng and Xin Wang for their helpful discussion of microarray data analysis. We also thank Dorothea Dudek for her editorial and graphic assistance, and Irwin Arias for his critical review of the manuscript.

REFERENCES

1. Travis WD, Gal AA, Colby TV, et al: Reproducibility of neuroendocrine lung tumor classification. Hum Pathol 29:272-279, 1998

2. Travis WD, Rush W, Flieder DB, et al: Survival analysis of 200 pulmonary neuroendocrine tumors with clarification of criteria for atypical carcinoid and its separation from typical carcinoid. Am J Surg Pathol 22:934-944, 1998

3. Zacharias J, Nicholson AG, Ladas GP, et al: Large cell neuroendocrine carcinoma and large cell carcinomas with neuroendocrine morphology of the lung: Prognosis after complete resection and systematic nodal dissection. Ann Thorac Surg 75:348-352, 2003

4. Schena M, Shalon D, Davis RW, et al: Quantitative monitoring of gene expression patterns with a complementary DNA microarray. Science 270:467-470, 1995

5. DeRisi J, Penland L, Brown PO, et al: Use of a cDNA microarray to analyse gene expression patterns in human cancer. Nat Genet 14:457-460, 1996

6. Garber ME, Troyanskaya OG, Schluens K, et al: Diversity of gene expression in adenocarcinoma of the lung. Proc Natl Acad Sci U S A 98:13784-13789, 2001

7. Bhattacharjee A, Richards WG, Staunton J, et al: Classification of human lung carcinomas by mRNA expression profiling reveals distinct adenocarcinoma subclasses. Proc Natl Acad Sci U S A 98: 13790-13795, 2001

8. Miura K, Bowman ED, Simon R, et al: Laser capture microdissection and microarray expression analysis of lung adenocarcinoma reveals tobacco smoking- and prognosis-related molecular profiles. Cancer Res 62:3244-3250, 2002

9. Sugita M, Geraci M, Gao B, et al: Combined use of oligonucleotide and tissue microarrays identifies cancer/testis antigens as biomarkers in lung carcinoma. Cancer Res 62:3971-3979, 2002

10. Jones MH, Virtanen C, Honjoh D, et al: Two prognostically significant subtypes of high-grade lung neuroendocrine tumours independent of small-cell and large-cell neuroendocrine carcinomas identified by gene expression profiles. Lancet 363:775-781, 2004

11. Emmert-Buck MR, Bonner RF, Smith PD, et al: Laser capture microdissection. Science 274:998-1001, 1996

12. Reddel RR, Ke Y, Gerwin BI, et al: Transformation of human bronchial epithelial cells by infection with SV40 or adenovirus-12 SV40 hybrid virus, or transfection via strontium phosphate coprecipitation with a plasmid containing SV40 early region genes. Cancer Res 48:1904-1909, 1988

13. Luo L, Salunga RC, Guo H, et al: Gene expression profiles of laser-captured adjacent neuronal subtypes. Nat Med 5:117-122, 1999

14. Eisen MB, Spellman PT, Brown PO, et al: Cluster analysis and display of genome-wide expression patterns. Proc Natl Acad Sci U S A 95:14863-14868, 1998

15. Gillett C, Fantl V, Smith R, et al: Amplification and overexpression of cyclin D1 in breast cancer detected by immunohistochemical staining. Cancer Res 54:1812-1817, 1994

16. Beasley MB, Lantuejoul S, Abbondanzo S, et al: The P16/cyclin D1/Rb pathway in neuroendocrine tumors of the lung. Hum Pathol 34:136-142, 2003

17. Sattler M, Salgia R: Molecular and cellular biology of small cell lung cancer. Semin Oncol 30:57-71, 2003

18. Mariani L, McDonough WS, Hoelzinger DB, et al: Identification and validation of P311 as a glioblastoma invasion gene using laser capture microdissection. Cancer Res 61:4190-4196, 2001

19. Walch AK, Zitzelsberger HF, Aubele MM, et al: Typical and atypical carcinoid tumors of the lung are characterized by 11q deletions as detected by comparative genomic hybridization. Am J Pathol 153:1089-1098, 1998

20. Finkelstein SD, Hasegawa T, Colby T, et al: 11q13 allelic imbalance discriminates pulmonary carcinoids from tumorlets: A microdissection-based genotyping approach useful in clinical practice. Am J Pathol 155:633-640, 1999

21. Michelland S, Gazzeri S, Brambilla E, et al: Comparison of chromosomal imbalances in neuroendocrine and non-small-cell lung carcinomas. Cancer Genet Cytogenet 114:22-30, 1999

22. Brambilla E, Negoescu A, Gazzeri S, et al: Apoptosis-related factors p53, Bcl2, and Bax in neuroendocrine lung tumors. Am J Pathol 149:1941-1952, 1996

23. Baylin SB, Esteller M, Rountree MR, et al: Aberrant patterns of DNA methylation, chromatin formation and gene expression in cancer. Hum Mol Genet 10:687-692, 2001

24. Xiang CC, Chen M, Kozhich OA, et al: Probe generation directly from small numbers of cells for DNA microarray studies. Biotechniques 34:386-383, 2003

25. Ohnuki Y, Reddel RR, Bates SE, et al: Chromosomal changes and progressive tumorigenesis of human bronchial epithelial cell lines. Cancer Genet Cytogenet 92:99-110, 1996

26. Staudt LM, Wilson WH: Focus on lymphomas. Cancer Cell 2:363-366, 2002

27. Manser E, Fernandez D, Loo L, et al: Human carboxypeptidase E: Isolation and characterization of the cDNA, sequence conservation, expression and processing in vitro. Biochem J 267:517-525, 1990

28. Naggert JK, Fricker LD, Varlamov O, et al: Hyperproinsulinaemia in obese fat/fat mice associated with a carboxypeptidase E mutation which reduces enzyme activity. Nat Genet 10:135-142, 1995

29. Wang Y, Nimec Z, Ryan TJ, et al: The properties of the secreted gamma-glutamyl hydrolases from H35 hepatoma cells. Biochim Biophys Acta 1164:227-235, 1993

30. Li WW, Waltham M, Tong W, et al: Increased activity of gamma-glutamyl hydrolase in human sarcoma cell lines: A novel mechanism of intrinsic resistance to methotrexate (MTX). Adv Exp Med Biol 338:635-638, 1993

31. Longo GS, Gorlick R, Tong WP, et al: Gamma-glutamyl hydrolase and folylpolyglutamate synthetase activities predict polyglutamylation of methotrexate in acute leukemias. Oncol Res 9:259-263, 1997

32. Rots MG, Pieters R, Peters GJ, et al: Role of folylpolyglutamate synthetase and folylpolyglutamate hydrolase in methotrexate accumulation and polyglutamylation in childhood leukemia. Blood 93:1677-1683, 1999

33. Petersen I, Langreck H, Wolf G, et al: Small-cell lung cancer is characterized by a high incidence of deletions on chromosomes 3p, 4q, 5q, 10q, 13q and 17p. Br J Cancer 75:79-86, 1997

34. Ullmann R, Petzmann S, Sharma A, et al: Chromosomal aberrations in a series of large-cell neuroendocrine carcinomas: Unexpected divergence from small-cell carcinoma of the lung. Hum Pathol 32:1059-1063, 2001